Precise Estimation of Painting Surfaces for Digital Archiving

Tetsushi Tanimoto, Takahiko Horiuchi, and Shoji Tominaga

Graduate School of Advanced Integration Science, Chiba University
Chiba, 263-8522 Japan
t_tanimoto@chiba-u.jp,
{horiuchi,shoji}@faculty.chiba-u.jp

Abstract. This paper proposes a method for precisely estimating the surface properties of oil paintings for digital archiving. The surface properties include surface height information, surface spectral reflectance, and reflection model parameters. We use mainly a multiband imaging system and a high-resolution RGB camera, and use locally a spectrometer and a laser-scanning meter for precise surface measurement. First, we combine the estimated surface-spectral reflectances in high resolution from the multiband system and the measurements in low resolution from the spectrometer. Second, we combine the estimated surface height in high resolution from the RGB camera and the measurements in low resolution from a laser-scanning meter. Third, we develop a region dependent rendering algorithm where appropriate reflection parameters are determined for classified regions. All estimates of the surface properties are combined for rendering realistic color images of oil paintings. The feasibility of the proposed methods is shown in experiments using real oil paintings.

Keywords: Color image rendering, precise color reproduction, oil painting, surface property estimation, digital archivingt.

1 Introduction

The old type of digital archiving of art paintings was called "viewpoint and illumination-specific digital archiving" [1], which achieved a pleasing record only for a single viewpoint and for a limited range of materials with minor surface height. The surface of an oil painting is not smooth, but rough. Because the surface material consists of a thick oil layer, strong glosses or specular highlights appear on the surface. Therefore, "viewpoint and illumination-independent digital archiving" is required for rendering art paintings at different viewpoints and illuminations.

The authors have been working on development of techniques for viewpoint and illumination independent digital archiving of oil paintings [2]-[3], in which the painting surface is regarded as a 2D rough surface with gloss and shading. The procedure for total digital archiving is divided into three steps: acquisition,

S. Tominaga, R. Schettini, and A. Trémeau (Eds.): CCIW 2013, LNCS 7786, pp. 171–183, 2013.

analysis, and rendering. The surface properties of oil paintings, including surface height information, surface spectral reflectance, and reflection model parameters, are required for realistic image rendering. However, the previous methods had three problems: (1) Surface spectral reflectance estimation does not provide accuracy good enough for vivid color or saturated color. (2) 3D surface reconstruction is not precise particularly for oil paints on a canvas texture. (3) Realistic images are not rendered using a reflection model with fixed parameters.

This paper proposes a method for precisely estimating the surface properties of oil paintings to overcome the abovementioned three limitations, and improve the quality of rendered images. The first problem (1) is caused by the transmittance property of color filters. For solving this, we classify the entire painting surface into several regions based on the estimated surface-spectral reflectances. Then, spectral reflectances in a surface region with low estimation accuracy are measured directly by using a spectrometer. The principal components are computed from the measured spectral reflectances. We replace the first three components from the estimates with the corresponding components from the measurements, so that color reproduction is improved in regions with high chroma.

The second problem (2) is based on uneven surface by canvas fabric or panel. For solving this, surface height is constructed from the surface normals estimated from high-resolution images. Then, we use the low-resolution surface height information from measurements by a laser scanning meter [4]. The accuracy of the constructed surface is then improved by incorporating the low-resolution height information to the high-resolution gradient images on the Fourier space.

The third problem (3) is caused by difference in thickness of oil paint layer. For solving this, we develop a region-dependent rendering algorithm where appropriate reflection parameters are determined for the classified regions. We use the Torrance-Sparrow model with the specular reflection parameters adjusted to the classified regions.

We propose a method for analysis and synthesis of oil paintings based on the above improvements. The feasibility of the proposed method is shown in experiments using a real oil painting.

2 Imaging System

Two imaging systems are developed for estimating surface properties. One is a multiband imaging system, and another is a high-resolution imaging system. The multiband imaging system is developed for estimating the surface-spectral reflectance function. This system is decomposed into a monochrome camera and a multispectral lighting system. The camera is a Toshiba camera with a 1636×1236 pixel size and a 10 bit quantization. The lighting system consists of a slide projector and six color filters. The combined system provides a stable imaging system with six spectral bands in the wavelength range of 400 to 700 nm. This system is used for estimating the spectral reflectance of a painting surface. The spectral reflectance is recovered using the Wiener estimator to the noisy sensor outputs [5].

Next, the high-resolution imaging system is developed for precisely estimating the surface normals of small facets on an oil painting. The camera is a Canon EOS camera with a 5634×3753 pixel size, RGB channels, and a 14-bit quantization level. The lighting system uses the same projector of a white light source without color filters. The estimates of surface orientation should not depend on the surface colors. Therefore, we fit the RGB spectral sensitivities, $R(\lambda)$, $G(\lambda)$, and $B(\lambda)$, to the CIE standard luminosity function $V(\lambda)$ of the human visual system as

$$V(\lambda) = c_1 R(\lambda) + c_2 G(\lambda) + c_3 B(\lambda). \tag{1}$$

Then, the camera output RGB values $\{r(x,y), g(x,y), b(x,y)\}$ at a pixel (x,y) are converted into the radiance values $l(x,y)$ as

$$l(x,y) = w(c_1 r(x,y) + c_2 g(x,y) + c_3 b(x,y), \tag{2}$$

where w is a scaling factor.

The spectrometer is used for measuring a ground-truth of spectral reflectances at certain points in a specific classified region with low reproduction. The spectrometer used in this paper is a GretagMachbeth Spectrolino which can measure a spectral reflectance with high accuracy. Although accurate spectral reflectance is measured directly, the spatial resolution is not high. Therefore, it is only available for measuring some points on a painting.

The laser scanning meter is used for obtaining surface height information. The meter used in this paper is a Keyence laser confocal displacement meter. A surface is scanned with high accuracy and resolution of 0.2 μm. Although accurate surface height is measured directly, there are some limitations. It takes too much time to measure even a small painting in high resolution. Therefore, it is only available for measuring accurate surface heights at a small number of locations.

3 Precise Estimation of Surface Spectral Reflectances

3.1 Spectral Reflectance Estimation

We estimate the surface-spectral reflectance function from 6-band image data captured by using the multiband imaging system. The sensor output can be written as

$$\rho_i = \int_{400}^{700} S(\lambda) E(\lambda) R_i(\lambda) d\lambda + n_i, \quad (i = 1, 2, \cdots, 6), \tag{3}$$

where $S(\lambda)$ is the surface spectral reflectance, $E(\lambda)$ is the spectral distribution function of the illumination. $R_i(\lambda)$ is the spectral sensitivity function of the i-th sensor, and i is the noise component with zero mean, including the image sensor noise and an approximation error in the model. $E(\lambda)$ and $R_i(\lambda)$ are assumed to be known in advance.

Assume that each spectral function is sampled at 61 points with an equal interval $\Delta\lambda$ (5 nm) in the region [400nm, 700nm]. Let $\mathbf{S}$ be a 61-dimensional column vector representing the spectral reflectance $S(\lambda)$, $\mathbf{H}$ be a 6×61 matrix with the element $h_{ij} = E(\lambda_j)R_i(\lambda_j)\Delta\lambda$, ρ be a 6D column vector representing the sensor outputs, and $\mathbf{n}$ be a 6D noise column vector. Then Eq. (3) is described in a matrix equation.

$$\rho = \mathbf{HS} + \mathbf{n}. \tag{4}$$

When the signal component $\mathbf{S}$ and the noise component $\mathbf{n}$ are uncorrelated, optimized solution is given by using Wiener estimation [6]:

$$\hat{\mathbf{S}} = \mathbf{C}_{SS}[\mathbf{H}\mathbf{C}_{SS}\mathbf{H}^T + \sigma^2\mathbf{I}]^{-1}\rho. \tag{5}$$

where σ^2 is the noise variance, $\mathbf{I}$ is a 61×61 unit matrix, and $\mathbf{C}_{SS}$ is an 61×61 covariance matrix. To determine $\mathbf{C}_{SS}$, we used a database of many surface-spectral reflectances for different paints.

3.2 Improved Spectral Reflectance Estimation

Estimation of surface spectral reflectances is based on the captured 6-band image data. Owing to the transmittance property of color filters, certain colors, especially in dark vivid colors, had low reproduction accuracy of spectral reflectance. So we propose a method for improving the spectral reflectances with low estimation accuracy by using the direct measurements. First, in order to extract spectral reflectances with low estimation accuracy, we classify the entire painting surface into several regions based on the estimated surface-spectral reflectances by the k-means algorithm [6],[7]. The k-means algorithm partitions N data points into K disjoint subsets C_k containing N_k data points so as to minimize the sum-of-squares criterion J,

$$J = \sum_{k=1}^{K}\sum_{n=1}^{N_k} |\mathbf{S}_n - \bar{\mathbf{S}}_k|^2, \tag{6}$$

where $\mathbf{S}_n$ and $\bar{\mathbf{S}}_k$ are estimated surface spectral reflectance vector and the geometric centroid in C_k. The initial seed points are assigned to $k = 1, 2, \cdots, K$ classes including the point which has spectral reflectance with low estimation accuracy, then the centroid is re-computed after clustering and the seed points are renewed. The renewal is continued unit no further change occurs in the centroid by iteration.

Next, spectral reflectances in a surface region with low estimation accuracy are measured directly by using the spectrometer as described in Sec. 2. The principal components $\{\hat{\mathbf{S}}_1, \hat{\mathbf{S}}_2, \cdots, \hat{\mathbf{S}}_n\}$ are computed from the measured spectral reflectances. In the same way, the principal components $\{\mathbf{S}_1, \mathbf{S}_2, \cdots, \mathbf{S}_n\}$ are computed from the estimated spectral reflectances in the surface region with low

estimation accuracy. In both estimates and measurements, the percent variances are more than 0.999 for the first three components. Therefore, we approximate the estimated spectral reflectances $\mathbf{S}'$ by the first three components:

$$\mathbf{S}' = w_1\mathbf{S}_1 + w_2\mathbf{S}_2 + w_3\mathbf{S}_3, \tag{7}$$

where, $\{w_1, w_2, w_3\}$ are weighting coefficients. Then, we replace the first three components $\{\mathbf{S}_1, \mathbf{S}_2, \mathbf{S}_3\}$ with the corresponding three components $\{\hat{\mathbf{S}}_1, \hat{\mathbf{S}}_2, \hat{\mathbf{S}}_3\}$ of the measurements. Then, by using the same weight coefficients, improved spectral reflectances $\hat{\mathbf{S}}^*$ are estimated as

$$\hat{\mathbf{S}}^* = w_1\hat{\mathbf{S}}_1 + w_2\hat{\mathbf{S}}_2 + w_3\hat{\mathbf{S}}_3. \tag{8}$$

4 Precise Estimation of Surface Shape

4.1 Estimation of Surface Normal

To reconstruct surface shape, the surface normal vector is estimated using a photometric stereo method [8]. The painting surface is observed at the nine illumination directions, which composite four directions at 60 degrees and 45 degrees angle of incidence for the oil painting, respectively, and one direction from the top of the oil painting. First, let $\mathbf{I} = [I_1, I_2, \cdots, I_9]$ be a 1×9 matrix of the observed radiance values at pixel point. For calibration, we use a standard white matt paper for correcting non-uniform illumination. The radiances for this standard are observed at the same nine directions. Then the illumination correction is done by dividing the radiances from the painting surface with the ones from the standard.

The assumption of diffuse reflection gives us the relationship $\mathbf{I} = \alpha\mathbf{N}^{\mathrm{T}}\mathbf{L}$, where $\mathbf{N}$ is a surface normal vector and $\mathbf{L}$ is a 3×9 matrix showing a set of illumination directional vectors. Therefore an estimate $\hat{\mathbf{N}}$ of the surface normal is obtained as the least squared solution $\hat{\mathbf{N}} = \mathbf{L}^{+\mathrm{T}}\mathbf{I}^{\mathrm{T}}$, where $\mathbf{L}^+$ is a generalized inverse of $\mathbf{L}$.

4.2 Improved Surface Height Estimation

Surface heights are recovered from the estimated normal vectors by using the consistent gradient operator [9],[10]. Surface heights inevitably suffer from low-frequency distortion, because of the surface-normal vectors estimated from the noisy and uneven surface of canvas fabric or panel. In this paper, we focus on the latter distortion. To solve this problem, a small number of direct measurements of surface height can be incorporated [11]. The precise height measurements are used for the low-frequency components of the reconstructed surface height. Figure 1 shows a conceptual diagram.

We measure the surface height at small number of location on a painting surface. In experiments, twenty-one locations are taken to be able to cover uneven

surface. To determine a smooth surface, these measurement points are interpolated using a 3rd order spline function. This surface image is placed on the $2^n \times 2^n$ extended plane in the same mirror arrangement as the above. A fast Fourier transform (FFT) algorithm provides low-frequency components of the surface basis.

On the other hand, we estimate surface height from the surface normals by using the Chellappa-like algorithm with the integrability and distortion reduction. This FFT provides reliable estimates of the surface height for the higher frequency part. Therefore, we discard the low-frequency part of this high-resolution height estimates, and substitute the low-frequency components of the direct measurements for the corresponding frequency part of the high-resolution estimates. The precise shape of a painting surface is reconstructed from an IFFT of the whole composite frequency components.

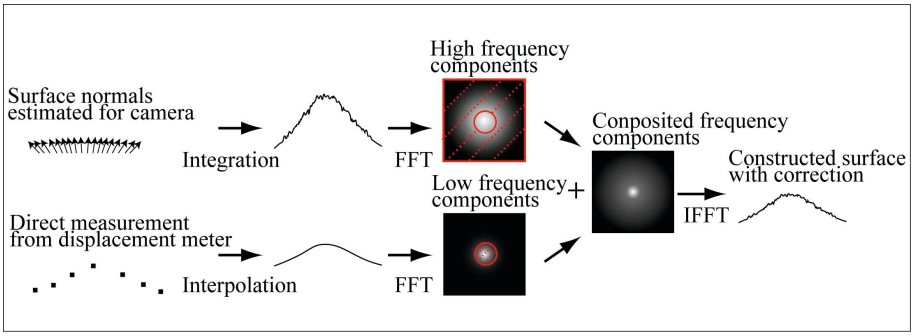

Fig. 1. Computational flow for accurate surface reconstruction

5 Realistic Image Rendering

5.1 Surface Reflectance Model

A 3D reflection model is important for analysis and synthesis of oil paintings. The Torrance-Sparrow model is used as the 3D reflection model in this study. In this model, a specular surface is assumed to be an isotropic collection of planar microscopic facet. The following vectors are defined for describing the model. Let $\mathbf{Q}$ be the normal vector of a microscopic facet and $\mathbf{N}$ be the normal vector of a macroscopic surface. Next, let $\mathbf{L}$ be the incident light vector (pointing towards the light source), and $\mathbf{V}$ be the view vector (pointing towards the viewer). The related angles are defined as follows: θ_i is the angle of incidence, θ_r is the viewing angle, ϕ is the angle between $\mathbf{N}$ and $\mathbf{Q}$, and θ_α is the angle of incidence to microfacet. Then the spectral radiance distribution at a spatial location is described as a function of the wavelength λ.

$$Y(\lambda) = \alpha \cos(\theta_i) S(\lambda) E(\lambda) + \beta \frac{D(\phi) G(\mathbf{N}, \mathbf{V}, \mathbf{L}) F(\theta_q, n)}{\cos(\theta_r)} E(\lambda), \tag{9}$$

$$D(\phi) = \exp\left\{ -\ln(2)\phi^2 / \gamma^2 \right\}, \tag{10}$$

where the first and second terms of the right-hand side represent, respectively, the body (diffuse) and interface (specular) reflection components. The second term of the interface reflection component consists of several terms. D is a distribution function. This function provides the index of surface roughness γ. A small value of γ is a geometrical attenuation factor. F represents the Fresnel spectral reflectance. The Fresnel equation provides the physically precise reflectance of interface-reflection.

5.2 Region-Dependent Rendering Parameters

Because of difference in thickness of oil paint layer, realistic images are not rendered using a reflection model with fixed parameters. We develop a region-dependent rendering algorithm where appropriate reflection parameters are determined for the classified regions.

First, we classify the entire painting surface into several regions. Even if the surface-spectral reflectance is the same, reflection properties such as the strength of a specular highlight may be different, depending on the thickness of oil paint layer. Therefore, we assume that adjacent pixels have almost the same thickness of the oil paint layer, and add the pixel location (x, y) as a spatial feature to the classification features of the k-means algorithm in Sec 3.2. Then, the k-means algorithm partitions N data points into K disjoint subsets C_k containing N_k data points so as to minimize the sum-of-squares criterion J,

$$J = \sum_{k=1}^{K} \sum_{n=1}^{N_k} |\mathbf{S}_n^* - \bar{\mathbf{S}}_k^*|^2, \tag{11}$$

where $\mathbf{S}_n^* = \{S^*(400), S^*(405), \cdots, S^*(700), \xi_x x, \xi_y y\}$, and ξ_x and ξ_y are weighting coefficients for the spatial feature.

Next, in order to represent various specular reflection properties accurately, we change the strength of specular reflection β, surface roughness γ, and index of reflection n in Eqs. (9) and (10) as

$$Y(\lambda) = \alpha \cos(\theta_i) S(\lambda) E(\lambda) + \beta_l \frac{D(\phi) G(\mathbf{N}, \mathbf{V}, \mathbf{L}) F(\theta_q, n_l)}{\cos(\theta_r)} E(\lambda), \tag{12}$$

$$D(\phi) = \exp\left\{ -\ln(2)\phi^2 / \gamma_l^2 \right\}, \quad (l = 1, 2, \cdots, L), \tag{13}$$

where L is the number of areas with different specular reflection property, and it is empirically determined.

6 Experiments

Figure 2 shows an example of oil painting called "Paris" in our collection of art paintings. The size is about 15.7×22.8 cm^2, and the surface is not flat but slightly uneven by canvas fabric. First, this painting was observed by the multiband imaging system resulting in an array of size of 1298×1883 pixels. Next, the painting was observed under nine illumination directions by the high-resolution RGB camera. The image size was 3313×4770 pixels, and the resolution was 47.6 μm/pixel.

Fig. 2. Test sample "Paris" of oil painting, where white circles show test 28 areas

6.1 Estimation Results of Spectral Reflectance

First, the surface spectral reflectances were estimated at all pixels from image data using the Wiener estimator described in Sec. 3.1. Table 1 shows the root mean square errors (RMSEs) between estimation results and measurements by spectrometer among 28 areas indicated in Fig. 2. Table 1 suggests that areas 1-9, which locates region of sky, have spectral reflectances with low estimation accuracy.

In order to improve the estimation accuracy, we classified the entire painting surface into several regions for extracting the region of sky, based on the estimated surface-spectral reflectances by using the k-means algorithm. The number of regions for the paint is experimentally determined as $K = 20$. Figure 3 shows the extracted regions of sky using the proposed method in Sec. 3. Next, the principal components were derived for areas 1-9 from the estimates and measurements, respectively. Figure 4 shows the first three principal components for both data sets. Finally, we replaced only the first three components from the estimates with the first three components from the measurements as described

in Sec. 3.2. Table 2 shows the RMSEs for areas 1-9. Figure 5 shows estimated surface-spectral reflectances and the ground truth by measurement. Black, blue and red curves show the measured reflectances, the estimated reflectances by the conventional algorithm and the estimated reflectances by the proposed method, respectively. Table 2 and Fig. 5 show that the estimation results were improved effectively using the proposed algorithm.

Table 1. RMSEs of spectral reflectances between estimation results using Wiener estimation and measurements using spectrometer

Area	1	2	3	4	5	6	7	8	9
RMSE	0.055	0.056	0.054	0.053	0.062	0.065	0.066	0.055	0.055

10	11	12	13	14	15	16	17	18	19
0.029	0.021	0.037	0.035	0.039	0.021	0.036	0.026	0.026	0.022

20	21	22	23	24	25	26	27	28	Average
0.037	0.021	0.013	0.010	0.036	0.021	0.017	0.024	0.020	0.037

Fig. 3. Extracted sky regions

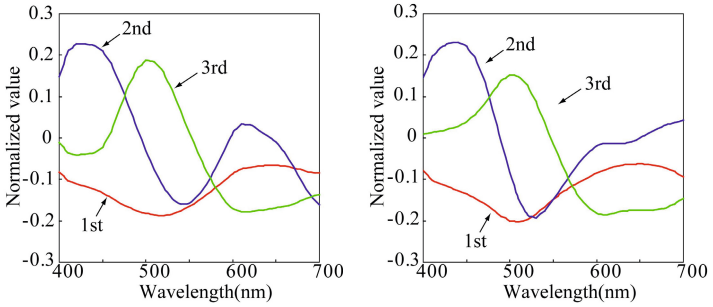

Fig. 4. First three principal components of the surface-spectral reflectances in the sky regions; (a) estimated data, (b) measured data

6.2 Estimation Results of Surface Shape

The surface normals at all pixel points were estimated by the photometric stereo from the diffuse reflection radiance data. First, the surface was constructed by performing the inverse FFT (IFFT) of the estimated surface heights. Figure 6(a) shows an image of the estimated 3D shape (red solid mesh) and the measured

Table 2. RMSEs between the estimates and the measurements in the sky areas

Area	1	2	3	4
RMSE(Conventional)	0.055	0.056	0.054	0.053
RMSE(Proposed)	0.049	0.048	0.035	0.034

5	6	7	8	9	Average
0.062	0.065	0.066	0.055	0.055	0.058
0.051	0.053	0.063	0.036	0.040	0.046

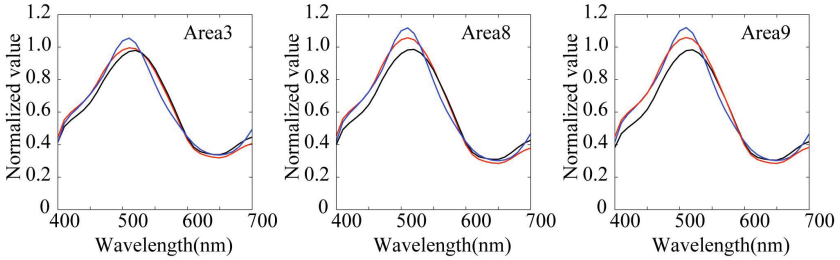

Fig. 5. Examples of surface-spectral reflectances within the sky regions (black curve: measured reflectances, blue curve: estimated reflectances by conventional algorithm, red curve: estimated reflectances by proposed method)

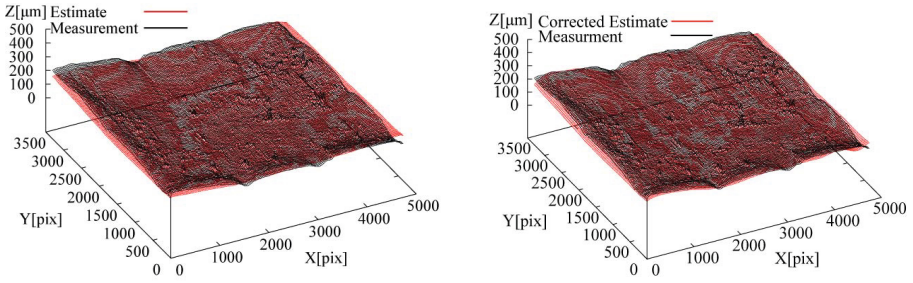

Fig. 6. Surface reconstruction results. (a) Conventional method (b) Proposed method.

(a)

(b)

(c)

Fig. 7. Rendering results: (a) Real photograph, (b)Rendered image by using the fixed rendering parameters for all regions, (c) Rendered image by the proposed region-dependent rendering algorithm

surface with laser scanning meter (black solid mesh). The average error was 21.7 μm. As shown in the figure, the estimated 3D shape does not represent precisely the uneven surface of canvas panel.

Next, surface height was measured at twenty-one locations of the painting surface. The low-frequency components were substituted for the corresponding part. Figure 6(b) depicts the reconstruction results with the additional low-resolution information. The average error is 12.0μm. The corrected estimates of the 3D shape are shown in red solid mesh, compared with the black solid mesh of the direct measurements. As shown in the figure, the corrected estimates can represent the uneven surface of canvas panel. The comparison suggests the improvement which results from incorporating a quite small number of measurements.

6.3 Rendering

Figure 7(a) shows the real photograph of "Paris". Figure 7(b) shows the rendered image under the same illumination conditions by using the fixed rendering parameters for all regions. The surface was illuminated by an artificial sunlight lamp with the incident angle of 80 degrees form the upper direction. As shown in Fig. 7(b), the stronger specular reflection region surrounded by a red curve in Fig. 7(a) was not recovered. In order to extract the region which has stronger specular reflection, we classified the entire painting surface into several regions by using the k-means algorithm described in Sec. 5.2. The number of regions for the paint is experimentally determined as $K = 20$.

In the rendering process, we set different parameters in Eqs. (12) and (13) for the region of strong specular reflection as $\beta_1 = 18.00$, $\gamma_1 = 0.020$ and $n_1 = 2.00$, and the other regions as $\beta_2 = 12.00$, $\gamma_2 = 0.012$ and $n_2 = 1.80$ empirically. Figure 7(c) shows the rendered image under the same illumination conditions as Fig. 7(a). By comparing Fig. 7(c) with the image in Fig. 7(b), the proposed method works well. The rendered image by the proposed method appropriately recovers strong specular reflection.

7 Conclusion

This paper has proposed a method for precisely estimating the surface properties of oil paintings for digital archiving. The surface properties included surface height information, surface spectral reflectance, and reflection model parameters. First, the surface spectral reflectances were estimated using the image data from the multiband system and the direct measurements from a spectrometer. Second, the surface heights were estimated using the image data from the RGB camera and the direct measurements from a laser-scanning meter. Third, the reflection model parameters were estimated depending on the classified region of a painting surface. All estimates of the surface properties were combined for rendering realistic color images. The feasibility of the proposed methods was shown in experiment using the oil painting of "Paris". The same experiment was performed to other oil paintings in our collection of art paintings, so that the proposed methods were effective for precisely estimating the surface properties.

References

1. Martinez, K., Cupitt, J., Saunders, D., Pillay, R.: Ten years of art painting research. Proc. of the IEEE 90(1), 28–41 (2002)
2. Tominga, S., Tanaka, N., Komada, T.: Imaging and rendering of oil paintings using multi-band camera. In: Proc. IEEE Southwest Symp. Image Anal. & Interpret, pp. 6–10 (2004)
3. Tominaga, S., Tanaka, N.: Spectral image acquisition, analysis, and rendering for art paintings. J. Electronic Imaging 17(4), 043022.1–043022.13 (2008)
4. Tominaga, S., Nishi, S.: Surface reflection properties of oil paints under various conditions. In: Proc. SPIE EI, vol. 6807, pp. 0M1–0M8 (2008)
5. Kay, S.: Fundamentals of statistical signal processing. Estimation Theory 12 (1993)
6. Forgy, E.: Cluster analysis of multivariate data: efficiency versus interpretability of classifications. Biometrics 21, 768–780 (1965)
7. MacQueen, J.: Some methods for classification and analysis of multivariate observations. In: Proc. 5th Berkeley Syp. on Math. Stat. and Prob. 1, pp. 281–297. Univ. of California Press, Berkerley (1967)
8. Woodham, R.: Photometric method for determining surface orientation from multiple images. Optical Engineering 19(1), 139–144 (1980)
9. Frankot, R., Chellappa, R.: A method for enforcing integrability in shape from shading algorithms. IEEE Trans. on PAMI 10(4), 439–451 (1988)
10. Ando, S.: Consistent gradient operator. IEEE Trans. on PAMI 22(3), 252–265 (2000)
11. Tominaga, S., Ujike, H., Horiuchi, T.: Surface reconstruction of oil paintings for digital archiving. In: Proc. IEEE southwest Symp. Image Anal. & Interpret, pp. 173–176 (2010)